ADV MATH SCI JOURNAL
Advances in Mathematics: Scientific Journal **9** (2020), no.11, 9259–9271
ISSN: 1857-8365 (printed); 1857-8438 (electronic)
https://doi.org/10.37418/amsj.9.11.31 Spec. Iss. on ICMMSIS-2020

MHD FLOW OF AN EYRING-POWELL FLUID WITH THE EFFECT OF THERMAL RADIATION, JOULE HEATING AND VISCOUS DISSIPATION

K. RAMESH BABU[1], G. NARENDER, AND K. GOVARDHAN

ABSTRACT. A two-dimensional stream of an magnetohydrodynamics (MHD) Eyring-Powell fluid on a stretching surface in the presence of thermal radiation, viscous dissipation and the Joule heating is analyzed. The flow model in the form of the Partial Differential Equations (PDEs) is transformed into a system of non-linear and coupled Ordinary Differential Equations (ODEs) by implementing appropriate similarity transformations. The resulting ordinary differential equations are solved numerically by the shooting technique with Adams-Moulton Method of fourth order. The numerical solution obtained for the velocity and temperature profiles has been presented through graphs for different choice of the physical parameters. The magnetic field is found to have a direct relation with the temperature profile and an inverse with the velocity profile. Increasing the thermal radiation, the temperature tends to rise.

1. INTRODUCTION

An Eyring-Powell fluid is an important subclass of non-Newtonian fluid. This kind of fluids are further classified into differential types, the integral models and shear rate models. Eyring-Powell fluid has distinct preference over the power-law model and depends on the kinetic theory of liquids. Newtonian behaviors f this fluid decrease for the low and high shear rates. These fluids are quite valuable for their application in many engineering, manufacturing and industrial areas such as pulp, plasma and other biological technology. Besides

[1]*corresponding author*

2020 *Mathematics Subject Classification.* 65M25, 76D05.

Key words and phrases. MHD, Eyring-Powell fluid, Thermal Radiation Parameter, Viscous Dissipation, speed slip parameter.

this, these fluids have essential aspects in fermentation, boiling, bubbles, column, plastic foam processing and in many more with substances such as mud, dyes, toothpaste, blood, corn starch, custard and honey being a few trivial examples of the non- Newtonian fluids. Eldabe et al. [1] elaborated the impact of isochoric non- Newtonian fluid flow by using the Eyring-Powell fluid model. Khan et al. [2] investigated the heat transfer flow of a fluid with the existence of warm radiation towards a circular stretching sheet. Rahimi et al. [3] resorted to the method of collocation for the solution of fluid with the boundary layer flow in an unbounded domain.

The study of the properties of the magnetic field and electrically conducting fluid is known as magnetohydrodynamics. The fundamental examples of magnetofluids are saltwater, liquid metals, plasmas and electrolytes. Hina [4] who discussed the work on magnetohydrodynamics on the peristaltic motion of Eyring-Powell with the consequence of warm and mass exchange and analyzed that by increment in the warm exchange coefficient, the temperature is also increased whereas the heat transfer coefficient is decreased by an increment in the magnetic field strength. The impact of MHD and nonlinear thermal radiation on an Eyring-Powell fluid over a permeable stretching surface was observed by Bhatti et al. [5]. They analyzed that the fluid motion is decreasing by an increment in the magnetic field. Babu et al. [6] analyzed the mass transfer flow for an Eyring-Powell fluid with the variation of magnetic field on a permeable expanding sheet. Narayana et al. [7] focused on the numerical study of two dimensional Eyring-Powell fluid with the impact of magnetohydrodynamics and heat transfer flow through a linear stretchable surface. Hayat et al. [8] worked on the magnetic nanoparticles for a radiative flow of an Eyring-Powell fluid by including thermophoresis and Brownian motion. The flow is assumed to pass through a stretching cylinder with the effect of convection. The influence of Biot number on the temperature field has been observed in this article. Mahanthesh et al. [9] inspected the time dependent threedimensional stream towards a stretchable sheet with the effect of Joule heating and thermal radiation. The shooting technique has been used for computing the numerical results.

The main objective of this article is to study the comprehensive review of Hayat et al. [10] and has been extended by considering the MHD boundary layer stream of the Eyring-Powell liquid on the extending sheet within the existence of warm radiation and Joule warming.

2. Mathematical Modeling

A 2D stream of an MHD Eyring-Powell liquid on an extending surface has been considered. The x-and y-axes are assumed to be along and opposite to the surface, respectively. The magnetic field B_0 acts in the y direction. A schematic diagram of the geometry is shown by Figure 1. The sheet is stretching on x-axis with speed $u_w = bx$ whereas b is a stretching constant.

The governing PDEs are:

$$\frac{\partial u}{\partial x} + \frac{\partial v}{\partial y} = 0, \tag{2.1}$$

$$u\frac{\partial u}{\partial x} + v\frac{\partial u}{\partial y} = \left(\nu + \frac{1}{\rho\beta C}\right)\left(\frac{\partial^2 u}{\partial x^2} + \frac{\partial^2 u}{\partial y^2}\right) - \frac{1}{2\rho\beta C^3}\left(\frac{\partial u}{\partial y}\right)^2 \frac{\partial^2 u}{\partial y^2} - \frac{\sigma B_0^2}{\rho}u, \tag{2.2}$$

$$u\frac{\partial T}{\partial x} + \mathrm{v}\frac{\partial T}{\partial y} = \frac{k}{\rho c_p}\left(\frac{\partial^2 T}{\partial x^2} + \frac{\partial^2 T}{\partial y^2}\right) - \frac{\nu}{\rho c_p}\left(\frac{\partial u}{\partial y}\right)^2 - \frac{1}{\rho c_p}\frac{\partial q_r}{\partial y} + \frac{\sigma B_0^2}{\rho c_p}u^2. \tag{2.3}$$

In equations (2.1)-(2.3), T denotes the temperature, ν the kinematic consistency, σ presents the conductivity of the fluid, ρ the liquid thickness while β and C are the aspects of an Eyring-Powell model. The parameters k represent the warm conductivity, c_p depicts specific heat of liquid and q_r represents the thermal radiation, are taken as constants.

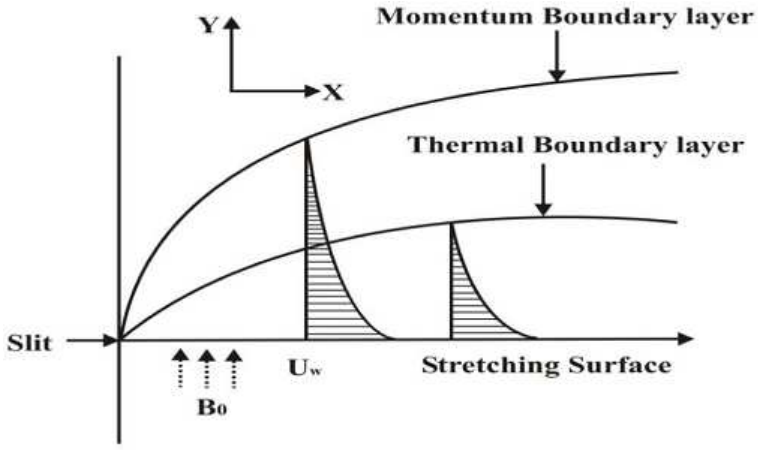

FIGURE 1. Schematic diagram of the physical problem

The associated BCs are:

$$\left.\begin{array}{l} \text{At } y=0: \quad u=u_w(x)=bx: \quad v=v_w, \ -k\frac{\partial T}{\partial y}=h_f(T_f-T) \\ \text{At } y\to\infty: \quad u\to 0, \ T\to T_\infty \end{array}\right\} \tag{2.4}$$

The v_w is taken as the mass transfer constant. In case of injection v_w is taken as a positive number while for suction case it is less than zero.

Now the stream function ψ has been introduced which is assumed to satisfy the continuity equation as below.

$$u=\frac{\partial\psi}{\partial y}, \quad v=-\frac{\partial\psi}{\partial x}$$

For the conversion of (2.1) - (2.3) into the dimensionless form, we present the taking after similitude change:

$$\psi=(a\nu)^{1/2}\,x\,f(\eta)$$

$$\eta=\left(\frac{a}{\nu}\right)^{1/2}y$$

$$\theta(\eta)=\frac{T-T_\infty}{T_f-T_\infty}$$

$$\left.\begin{array}{llll} \varepsilon=\frac{1}{\mu\beta C}, & \delta=\frac{a^3x^2}{2C^2\nu}, & \Pr=\frac{\mu C_p}{\kappa}, & M^2=\frac{\sigma B_0^2}{\rho a}, \quad R=\frac{4\sigma^* T_\infty^3}{k^* k} \\ S=-\frac{\nu_w}{\sqrt{a\nu}}, & \alpha=\frac{b}{a}, & Bi=\frac{h_f}{k}\sqrt{\frac{\nu}{a}}, & Ec=\frac{u_w^2}{C_p(T_w-T_\infty)} \end{array}\right\}$$

The final dimensionless form of the governing model is

$$(1+\varepsilon)h'''-\varepsilon\delta h'''(h'')^2-(h')^2+hh''-M^2h'=0$$

$$\frac{\left(1+\frac{4}{3}R\right)}{Pr}\theta"+h\theta'+M^2Ec(h')^2+Ec(h")^2=0.$$

The associated boundary conditions (2.4) take the form:

$$\left.\begin{array}{l} \text{At } \eta=0: \quad h(\eta)=S, \ \ h'(\eta)=\alpha, \ \ \theta'(\eta)=-Bi(1-\theta(0)) \\ \text{At } \eta\to\infty: \quad h'(\eta)\to 0, \ \theta(\eta)\to 0 \end{array}\right\}$$

The surface drag coefficient, is defined as:

$$C_{fx}=\frac{\tau_w}{\rho u_w^2},$$

where the surface drag coefficient at the wall is given by

$$\tau_w=\left(\mu+\frac{1}{\beta C}\right)\left(\frac{\partial u}{\partial y}\right)_{y=0}-\frac{1}{6\beta}\left(\frac{1}{C}\left(\frac{\partial u}{\partial y}\right)_{y=0}\right)^{3.}$$

The surface drag coefficient in the dimensionless form is given by

$$(Re_x)^{1/2} C_{fx} = (1+\varepsilon) h^{"}(0) - \frac{1}{3}\varepsilon\,\delta\,\left(h^{"}(0)\right)^3,$$

where the Reynolds number is given as

$$Re_x = \frac{ax^2}{\nu}.$$

The rate of heat transfer Nu_x is characterized by:

$$Nu_x = \frac{xq_w}{k(T_w - T_\infty)},$$

where

$$q_w = -\left(k + \frac{16\sigma^* T_\infty^3}{3k^*}\right)\left(\frac{\partial T}{\partial y}\right)_{y=0}.$$

The dimensionless form of the Nu_x, is

$$(Re_x)^{-1/2} Nu_x = -\left(1 + \frac{4}{3}R\right)\theta'(0).$$

3. Numerical Treatment

In our work we used shooting method to solve the transformed ODEs together with defined the boundary condition. For the implementation of the shooting method we first convert the system of equations into first order ODEs as follows:

Let us use the notations:

$$h = g_1,\ h' = g_2,\ h" = g_3,\ \theta = g_4,\ \theta" = g_5.$$

The system of first order ODEs are given as:

$$\begin{aligned}
g_1' &= g_2, & g_1(0) &= S,\\
g_2' &= g_3, & g_2(0) &= \alpha,\\
g_3^1 &= \frac{[Mg_2 + g_2^2 - g_1 g_3]}{1+\varepsilon-\varepsilon\delta g_3^2}, & g_3(0) &= p,\\
g_4' &= g_5, & g_4(0) &= q,\\
g_5^1 &= -\frac{\Pr}{\left(1+\frac{4}{3}R\right)}\left[g_1 g_5 + M^2 Ec\, g_2^2 + Ecg_3^2\right], & g_5(0) &= -Bi(1-q).
\end{aligned}$$

Because the numerical computations cannot be performed on an unbounded domain, therefore the domain $[0, \eta_\infty]$ taken as $[0, \infty)$, where $\eta_\infty \in Z^+$ for which

the variations in the solution are negligible after $\eta = \eta_\infty$. The ideal missing conditions p and q are iteratively updated by Newton's technique as follows

$$\begin{pmatrix} p^{(k+1)} \\ q^{(k+1)} \end{pmatrix} = \begin{pmatrix} p^k \\ q^k \end{pmatrix} - \begin{pmatrix} \frac{\partial g_2}{\partial p} & \frac{\partial g_2}{\partial q} \\ \frac{\partial g_4}{\partial p} & \frac{\partial g_4}{\partial q} \end{pmatrix}^{-1}_{\left(p^k, q^k, \eta_\infty\right)} \begin{pmatrix} g_2 \\ g_4 \end{pmatrix}_{\left(p^k, q^k, \eta_\infty\right)}.$$

The following new variables have been introduced for the further proceedings

$$\frac{\partial g_1}{\partial p} = g_6,\ \frac{\partial g_2}{\partial p} = g_7,\ \frac{\partial g_3}{\partial p} = g_8,\ \frac{\partial g_4}{\partial p} = g_9,\ \frac{\partial g_5}{\partial p} = g_{10},$$
$$\frac{\partial g_1}{\partial q} = g_{11},\ \frac{\partial g_2}{\partial q} = g_7,\ \frac{\partial g_3}{\partial p} = g_{13},\ \frac{\partial g_4}{\partial q} = g_{14},\ \frac{\partial g_5}{\partial q} = g_{15}.$$

By inserting these notations in the above Newton's iterative formulation, we get the form:

$$\begin{pmatrix} p^{(k+1)} \\ q^{(k+1)} \end{pmatrix} = \begin{pmatrix} p^k \\ q^k \end{pmatrix} - \begin{pmatrix} g_7 & g_{12} \\ g_9 & g_{14} \end{pmatrix}^{-1}_{\left(p^k, q^k, \eta_\infty\right)} \begin{pmatrix} g_2 \\ g_4 \end{pmatrix}_{\left(p^k, q^k, \eta_\infty\right)}.$$

The stopping criteria for the iterative procedure has been ready as:

$$\max\left\{\left|g_2\left(\eta_\infty\right)\right|,\ \left|g_4\left(\eta_\infty\right)\right|\right\} \leq \xi,$$

where ξ is a small positive number. For the computational purpose, ξ has been given the value $\xi = 10^{-8}$ whereas η_∞ is set as 8.

4. Tabular and Graphical Results

Table 1 shows the behaviors of $\varepsilon, \delta, \mathrm{Pr}, S, Bi, M, Ec$ and R on the skin friction and Nusselt number. By increasing the physical parameter ξ both the drag coefficient and the heat transfer increase. Increasing the values of δ, the skin friction and Nusselt number are observed to decrease. Increasing the values of Pr gives no effect on the surface drag coefficient while the rate of heat transfer increases with an increment in the Prandtl number. By increasing S , there is also an increase in the values of drag coefficient and heat exchange rate. By increasing the Biot number Bi, there is no effect on the drag coefficient, but heat exchange rate goes to increase. By increasing the magnetic parameter M, the values of surface drag increases while those of rate of heat exchange decrease with an increment in M. By increasing the Ec there is a decrement in the values of drag coefficient. Increasing R also gives increase in the values of heat exchange.

TABLE 1. Numerical outcomes of $(Re_x)^{1/2}\ C_{fx}$ and $(Re_x)^{-1/2}\ Nu_x$ for distinctive parameters when $\alpha = 0.5$.

ε	δ	Pr	S	Bi	M	Ec	R	$(Re_x)^{1/2}C_{fx}$	$(Re_x)^{-1/2}Nu_x$
0.2	0.2	1	0.5	1	0.2	0.1	0.1	0.54633560	0.46106580
0.3								056204120	0.46361050
0.5								0.59196700	0.46789060
1.0								0.65999860	0.41954190
0.3	0.1							0.54638200	0.46138360
	0.5							0.56156630	0.46389200
	1.0							0.56065780	0.46378720
	0.2	0.5						0.56193580	0.32088700
		1.2						0.56193580	0.50585760
		1.5						0.56193580	0.55782930
		1.0	0.2					0.47198170	0.37756690
			1.0					0.73742550	0.58079110
			1.0	0.5				0.73742550	0.38251270
				1.5				0.73742550	0.70210500
				1.5	0.3			0.75375260	0.70091000
					0.5			0.80276690	0.69738700
					0.5	0.2		0.80276690	0.68737420
						0.5		0.80276690	0.65733650
						0.5	0.2	0.80276690	0.69140920
							0.3	0.80276690	0.72203190

Figure 2 describes that by expanding the values of the liquid parameter ξ, there's an increase within the boundary layer thickness of the speed profile. Figure 3 shows the impact of the extending proportion parameter α on the speed and the boundary layer thickness which is related to it. It highlights the impact of the stretching ratio parameter α on the velocity profile. By this figure, it is clear that increasing α guides to an increment in the density of the velocity boundary layer. Figure 4 describes the impact of the suction parameter S on the speed $f^{'}(\eta)$. The suction parameter S and the speed $f^{'}(\eta)$ are noticed to have an inverse connection. An increase within the values of S causes a diminishment within the boundary layer thickness of the speed. Figure 5 describes the impact

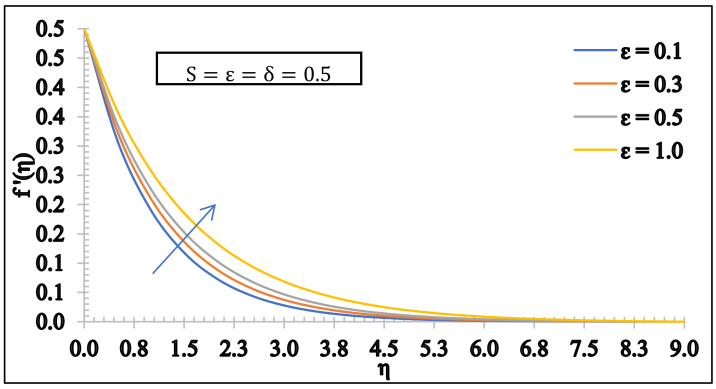

FIGURE 2. Effect of ε on $f^{'}(\eta)$

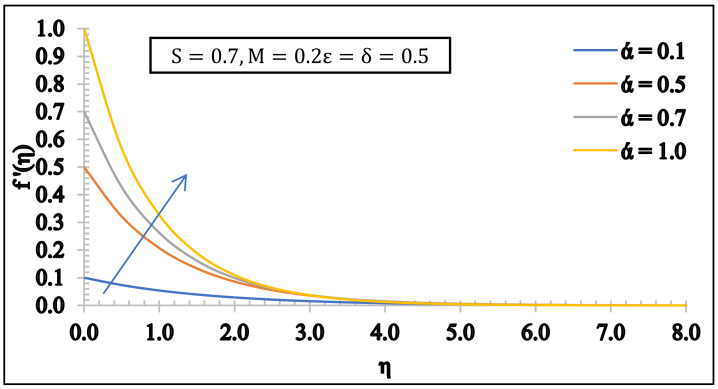

FIGURE 3. Effect of α on $f^{'}(\eta)$

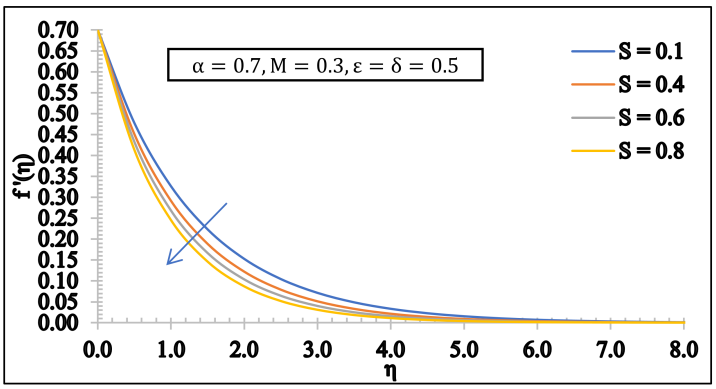

FIGURE 4. Effect of S on $f^{'}(\eta)$

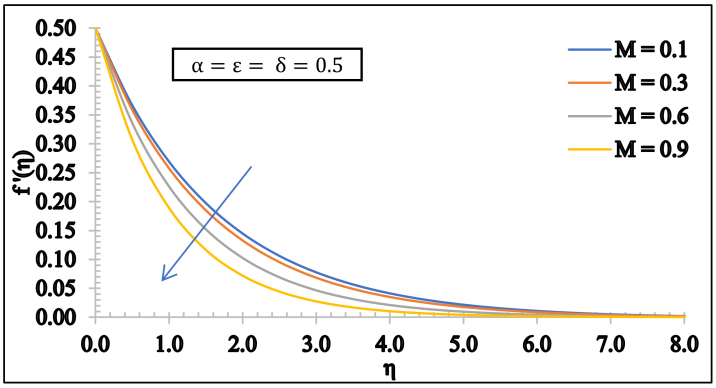

FIGURE 5. Effect of M on $f^{'}(\eta)$

of M on the speed profile which demonstrates that by expanding the values of M, the speed goes to diminish and the boundary layer thickness could be a diminishing function of M.

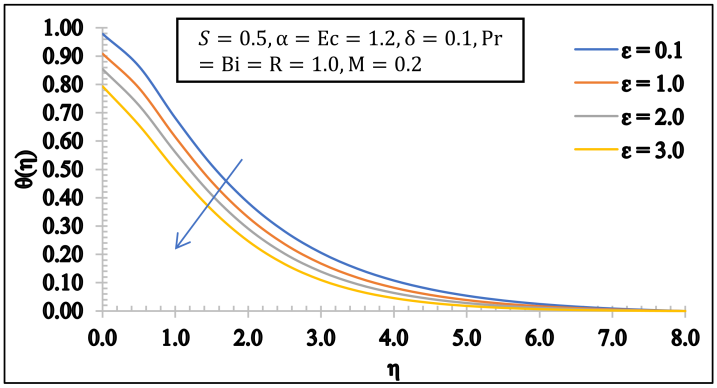

FIGURE 6. Effect of ε on $\theta(\eta)$

Figures 6 - 12 show the effects of distinctive parameters, $\varepsilon, S, M, \Pr, Ec, R$ and Bi on the energy profile.

Figure 6 gives the impact of ε on the energy. By expanding the characters of this material fluid parameter, the temperature goes to decrease. It has an inverse relation with the temperature. Figure 7 represents the influence of the suction parameter S on the temperature distributions. The temperature goes to decrease as we increase the values of S. The impact of M on the temperature distribution is presented in Figure 8. By expanding values of the M where the temperature

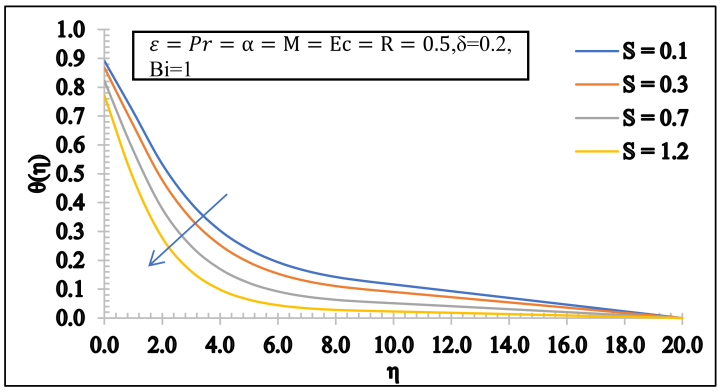

FIGURE 7. Effect of S on $\theta(\eta)$

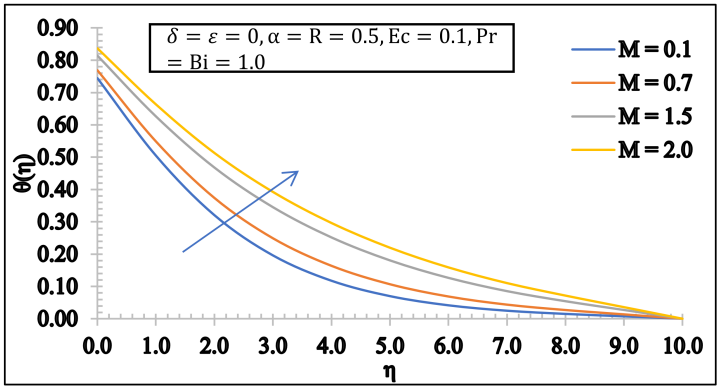

FIGURE 8. Effect of M on $\theta(\eta)$

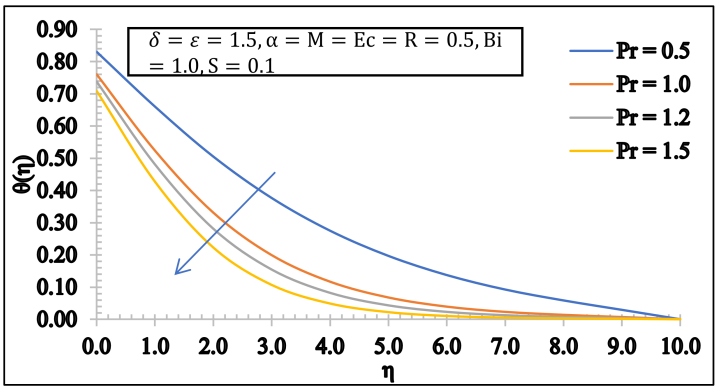

FIGURE 9. Effect of Pr on $\theta(\eta)$

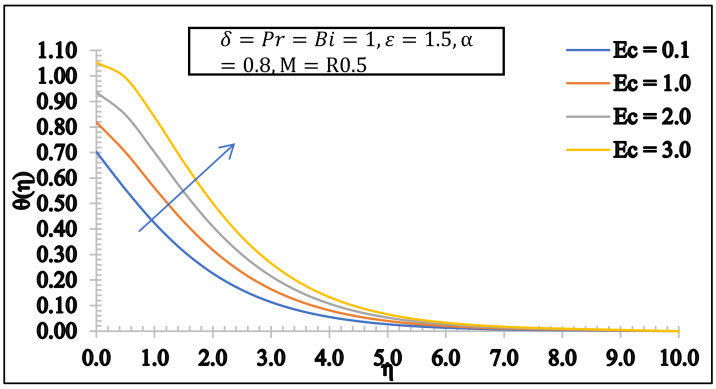

FIGURE 10. Effect of Ec on $\theta(\eta)$

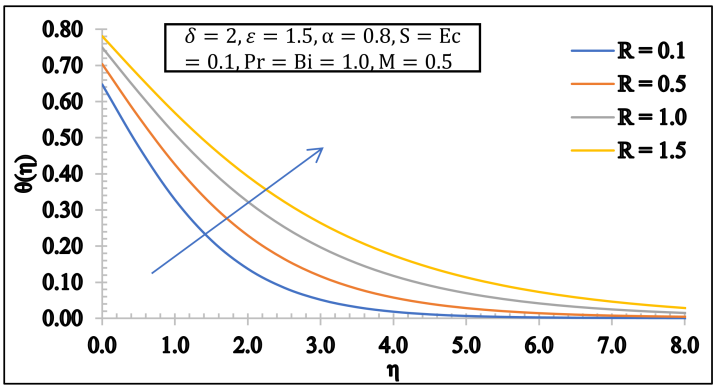

FIGURE 11. Effect of R on $\theta(\eta)$

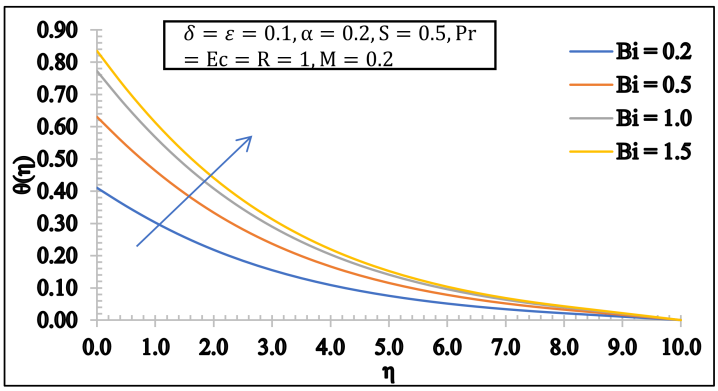

FIGURE 12. Effect of Bi on $\theta(\eta)$

profile is enhanced. From figure 9, gives the evident that increasing values of Prandtl number, the thermal diffusivity starts decreasing. So, for higher values of the Prandtl number results a strong reduction in temperature field. Figure 10 and 11 show the influence of Eckert number and radiation parameter R on the temperature distribution. It is seen that for gradually enhancing values of Ec and R energy profile also increased. These are increasing functions of temperature. Figure 12 is presented to visualize the effect of the Bi on temperature distribution. This figure defines that temperature profile enhances as the Biot number Bi is increased gradually.

CONCLUSION

Concluding all arguments and results we summarized our findings as follows: Enhancing the values of S , the velocity profile and the temperature profile tends to increase. Increased velocity profile while reduced temperature plots has been discovered for the ε. Decrement in temperature profile id observed for increasing the values of the Prandtl number. Because of strong magnetic field M causes increment in temperature profile and diminish velocity. Increasing the thermal radiation, the temperature tends to rise. Uprising of energy field is observed for the increasing value of Eckert number. The skin friction is increasing for the increment of ε and decreasing for the increment of δ.

REFERENCES

[1] N. ELDABE, A. HASSAN, M.A. MOHAMED:*Effect of couple stresses on the MHD of a non-Newtonian unsteady flow between two parallel porous plates*, Zeitschrift four Naturforschung A. **58**(4) (2003), 204–210.

[2] S.U. KHAN, N. ALI, Z. ABBAS: *Hydromagnetic flow and heat transfer of Eyring-Powell fluid over an oscillatory stretching sheet with thermal radiation*, Applications & Applied Mathematics, **10**(2) (2015).

[3] J.RAHIMI, D. GANJI, M. KHAKI, K. HOSSEINZADEH:*Solution of the boundary layer flow of an Eyring-Powell non-Newtonian fluid over a linear stretching sheet by collocation method*, Alexandria Engineering Journal, **56**(4) (2017), 621–627.

[4] S. HINA: *MHD peristaltic transport of Eyring-Powell fluid with heat/mass transfer, wall properties and slip conditions*, Journal of Magnetism and Magnetic Materials. **404** (2016), 148–158.

[5] M. BHATTI, T. ABBAS, M. RASHIDI, M. ALI, Z. YANG: *Entropy generation on MHD Eyring-Powell nanofluid through a permeable stretching surface*, Entropy, **18**(6) (2016), art.no.224.

[6] D.H. BABU, M.S. BABU, P. NARAYANA: *MHD mass transfer flow of an Eyring-Powell fluid over a stretching sheet*, Materials Science and Engineering Conference Series. **263**(6) (2017), 062013.

[7] P.S. NARAYANA, N. TARAKARAMU, S. MOLIYA AKSHIT, J. GHORI: *MHD flow and heat transfer of an Eyring-Powell fluid over a linear stretching sheet with viscous dissipation, A numerical study*, Frontiers in Heat and Mass Transfer, **9**(1) (2017), 1-5.

[8] T. HAYAT, M.I. KHAN, M. WAQAS, A. ALSAEDI: *Effectiveness of magnetic nanoparticles in radiative flow of Eyring-Powell fluid*, Journal of Molecular Liquids, **231** (2017), 126–133.

[9] B. MAHANTHESH, B. GIREESHA, R.S.R. GORLA: *Unsteady threedimensional MHD flow of a nano Eyring-Powell fluid past a convectively heated stretching sheet in the presence of thermal radiation, viscous dissipation and Joule heating*, Journal of the Association of Arab Universities for Basic and Applied Sciences, **23**(1) (2017), 75–84.

[10] T. HAYAT, Z. IQBAL, M. QASIM, A. ALSAEDI: *Flow of an Eyring-Powell fluid with convective boundary conditions*, Journal of Mechanics, **29**(9) (2013), 217–224.

DEPARTMENT OF MATHEMATICS
UNIVERSITY COLLEGE OF ENGINEERING, OSMANIA UNIVERSITY
HYDERABAD, TELANGANA STATE, INDIA.
Email address: ramesh.kasba@gmail.com

DEPARTMENT OF HUMANITIES AND SCIENCES (MATHEMATICS)
CVR COLLEGE OF ENGINEERING
HYDERABAD, TELANGANA STATE, INDIA.
Email address: gnriimc@gmail.com

DEPARTMENT OF MATHEMATICS
GITAM UNIVERSITY
HYDERABAD, TELANGANA STATE, INDIA.
Email address: govardhan_kamatam@yahoo.co.in